THOUGHTS AND PROGRESS

Ultrasound-based estimation of remaining cardiac function in LVAD-supported ex vivo hearts

Louis S. Fixsen[1] | Niels J. Petterson[1] | Patrick Houthuizen[2] |
Marcel C. M. Rutten[1] | Frans N. van de Vosse[1] | Richard G. P. Lopata[1]

[1]Cardiovascular Biomechanics group, Department of Biomedical Engineering, Eindhoven University of Technology, Eindhoven, The Netherlands

[2]Department of Cardiology, Catharina Hospital, Eindhoven, The Netherlands

Correspondence
Louis S. Fixsen, Cardiovascular Biomechanics group, Department of Biomedical Engineering, Eindhoven University of Technology, P.O. Box 513, GEM-Z4.11, 5600 MB Eindhoven, The Netherlands.
Email: l.s.fixsen@tue.nl

Abstract

Left ventricular assist devices (LVAD) provide cardiac support to patients with advanced heart failure. Methods that can directly measure remaining LV function following device implantation do not currently exist. Previous studies have shown that a combination of loading (LV pressure) and deformation (strain) measurements enables quantitation of myocardial work. We investigated the use of ultrasound (US) strain imaging and pressure–strain loop analysis in LVAD-supported hearts under different hemodynamic and pump unloading conditions, with the aim of determining LV function with and without LVAD support. Ex vivo porcine hearts (n = 4) were implanted with LVADs and attached to a mock circulatory loop. Measurements were performed at hemodynamically defined "heart conditions" as the hearts deteriorated from baseline. Hemodynamic (including LV pressure) and radio-frequency US data were acquired during a pump-ramp protocol at speeds from 0 (with no pump out-flow) to 10 000 revolutions per minute (rpm). Regional circumferential (ε_{circ}) and radial (ε_{rad}) strains were estimated over each heart cycle. Regional ventricular dys-synchrony was quantitated through time-to-peak strain. Mean change in LV pulse pressure and ε_{circ} between 0 and 10 krpm were −21.8 mm Hg and −7.24% in the first condition; in the final condition −46.8 mm Hg and −19.2%, respectively. ε_{rad} was not indicative of changes in pump speed or heart condition. Pressure–strain loops showed a degradation in the LV function and an increased influence of LV unloading: loop area reduced by 90% between 0 krpm in the first heart condition and 10 krpm in the last condition. High pump speeds and degraded condition led to increased dyssynchrony between the septal and lateral LV walls. Functional measurement of the LV while undergoing LVAD support is possible by using US strain imaging and pressure–strain loops. This can provide important information about remaining pump function. Use of novel LV pressure estimation or measurement techniques would be required for any future use in LVAD patients.

KEYWORDS

echocardiography, ex vivo heart, heart failure, left ventricular assist devices, pressure–strain loops, speckle tracking

---

1 | INTRODUCTION

Left ventricular (LV) assist devices (LVADs) are implants that provide an important alternative therapy for patients with end-stage heart failure when a heart transplant is either not available or not possible. LVADs provide mechanical circulatory support (MCS) by supplementing or replacing left ventricular function in supplying blood to the body. LVAD therapy is given based on clinical need and usually with one of three strategies in mind: as a bridge to heart transplantation; as a destination therapy[1]; or as a bridge to recovery, whereby a patient's residual cardiac function recovers sufficiently during therapy for the device to be explanted. Although this strategy is currently only attempted in a small number (1-3%) of LVAD patients worldwide,[2] studies that focused on recovery found that 5-24% of patients had recovered sufficiently for the explantation to take place.[3]

The cardiac function of MCS patients is monitored through the NYHA and INTERMACS classification systems and the use of echocardiography.[1,4] Echocardiographic measurements include the determination of aortic valve insufficiency and left ventricular ejection fraction. These measures are combined with patient symptoms, clinical observations and current medication, 6-minute walk distance,[5] or cardio-pulmonary exercise tests[6] to determine a patient's current cardiac health. However, clinicians currently lack intricate knowledge of the heart postimplantation, such as its ability to perform work. Invasive ventricular pressure measurements made using catheterization can lead to complications such as infection[7] and are generally not accepted as a standard diagnostic tool. Noninvasive diagnostic imaging methods for determining cardiac function such as tagged magnetic resonance imaging-based strain estimation and computed tomographic imaging are not possible in all patients for safety reasons.[8]

Echocardiography is presently used throughout the treatment of MCS patients.[9–13] Ultrasound strain imaging (or speckle tracking) is a technique that can determine motion or deformation within the heart. Since its introduction, US strain imaging has been applied to the estimation of left ventricular function,[14,15] including the use of time-to-peak strain in the estimation of left ventricular dyssynchrony.[16] However,

US strain imaging has yet to be validated for the monitoring of cardiac function in MCS patients.[17] Therefore, we undertook an investigation into the use of strain imaging in combination with MCS.

An experimental study involving a pump-ramp protocol was devised. Pump-ramp tests allow study of the effect of LVAD unloading on the heart.[6,11] The LVAD pump speed is increased from a minimum level through a range of speeds and the data are acquired when the heart is in a steady state. Experimental investigations allow for the control of the environment and hemodynamic measurements not usually available in patients, such as aortic and LV pressure. Studies on LVADs have previously been performed using mock loops.[18,19] Prior to this study, Pennings et al used an isolated beating heart setup to estimate LV pressure from pump flow and pressure.[20] More recently, the general use of such a setup for the validation of US-acquired parameters such as cardiac output and strain was shown in Petterson et al.[21]

In this study we investigated the use of ultrasound strain imaging for the determination of left ventricular function in the LVAD-supported heart. Ex vivo porcine hearts were implanted with LVADs, connected to a mock circulatory loop and imaged using ultrasound. Data were acquired at multiple time points as the hearts degraded from their baseline condition. At each condition, the relationship between pump speed, cardiac strains, and left ventricular pressure over the heart cycle was investigated. Analysis focused on the use of pressure–strain loops, which have been shown to directly relate to myocardial work and metabolism.[22,23] We demonstrate that through analysis of both pressure and strain the current ability of the heart to perform work while undergoing LVAD support can be understood.

2 | MATERIALS AND METHODS

2.1 | Ex vivo heart experiments

Four healthy porcine hearts were implanted with LVADs (Figure 1A) and connected to a mock circulatory loop (Figure 1B). The experimental setup has previously been
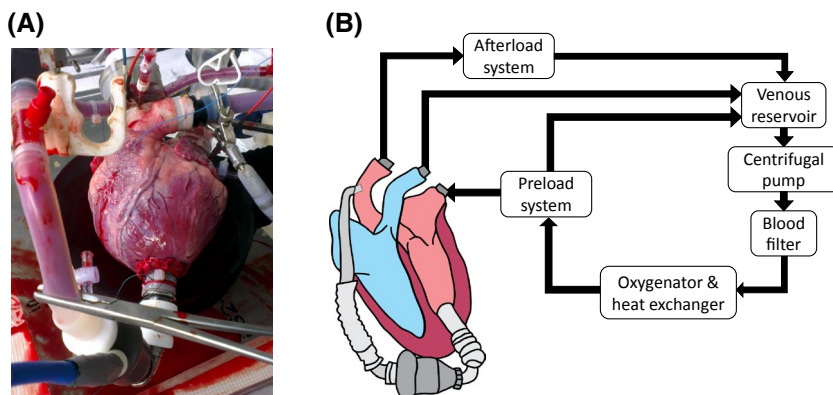
(A)

(B)

FIGURE 1 A, Ex vivo porcine heart with implanted left ventricular assist device (LVAD) at the apex. B, Schematic of experimental setup, showing ex vivo heart, with LVAD, connected to the mock systemic circulatory loop

detailed in Petterson et al and de Hart et al.[21,24] The hearts were obtained from Dutch landrace hybrid pigs intended for human consumption. The slaughterhouse and laboratory protocols were developed in accordance with EC regulations 1069/2009 regarding the use of slaughterhouse material for diagnosis and research, supervised by the Dutch Government (Dutch Ministry of Agriculture, Nature and Food Quality) and approved by the associated legal authorities of animal welfare (Food and Consumer Product Safety Authority).

In addition to the methods described in previous studies, the hearts were implanted with either MicroMed DeBakey (MMD, n = 2) or Thoratec HeartMate II (HM2, n = 2) LVADs, due to device availability constraints. Both devices were of an axial continuous-flow design with similar flow rates for each pump speed setting. The LVAD inflow cannula was positioned at the LV apex and fixed with a suture ring. The outflow was connected to the aorta, before the coronary arteries. Following LVAD implantation, the left side of the heart was connected to the mock systemic circulatory loop (PhysioHeart, Lifetec Group B.V., Eindhoven, The Netherlands) and reperfused with oxygenated blood. Blood was passed through an arterial filter prior to entering the left atrium (AFFINITY Arterial 38-µm blood filter, Medtronic, Dublin, Ireland) in order to remove any air bubbles. Additionally, any air build-up could be removed via valves at points throughout the mock loop. After reperfusion the heart would begin to contract in an uncontrolled manner and so was defibrillated to restore the full sinus rhythm. Once stable, the heart was immersed in saline heated to 38 °C for ultrasound imaging.

2.2 | Data acquisition

2.2.1 | Ultrasound

Two-dimensional time-resolved ultrasound data were acquired using MyLab70 XVG (Esaote Europe, Maastricht, The Netherlands) with a radiofrequency (RF) interface and CA431 curved array transducer (center frequency of 2.7 MHz). Ultrasound data were acquired up to a depth of 13

cm at a frame rate of 47 Hz. The probe was positioned to the side of the right ventricle so that a short-axis view of the left ventricle with the maximum field of view could be imaged. Long-axis views were not used due to the metal inflow cannula at the apex which created severe reverberation in the images. Reverberations cause artifacts in the image that lead to errors in the strain analysis, typically through anomalous high or low strains. True apical views were not possible due to the LVAD implanted at the apex, this also being the case in patients post-LVAD implantation.

Data were acquired at the mid-level of the heart, halfway between the apex and mitral valve, as shown in Figure 2A. The transducer was fixed to a rail and held in a clamp with multiple degrees of freedom for positioning. Acquisitions lasted approximately 10 seconds with an average 20 heart cycles of RF-data acquired. Figure 2B shows a representative B-mode image at end-diastole.

2.2.2 | Hemodynamics

Sensors in the aorta and left atrium measured pressure. Left ventricular pressure was measured via a venous catheter inserted through the ventricular wall at the apex. Cardiac output (CO) was calculated from the sum of coronary and systemic circulation flows and measured with clamp-on flow meters. These data were recorded at 1000 Hz. Datasets were categorized by so-called "heart condition", a relative definition of degradation for each heart. This was based on the reduction in CO and mean aortic pressure from baseline, which followed the nonischemic clinical scenario presented in.[25] At Heart condition I, 0 krpm, CO was typically close to 5 L/min, with a mean aortic pressure of 75–85 mm Hg, while in the most degraded condition (Heart condition II for the HM2 hearts and IV for MMD), CO was 3 L/min with a mean aortic pressure of 60 mm Hg. The number of complete datasets (heart conditions) per experiment depended on the rate at which each heart deteriorated, as well as the initial condition of each heart.

An initial measurement was made with the LVAD turned off and the pump outflow clamped shut. The pump speed was then varied between 7 and 10 thousand revolutions per minute
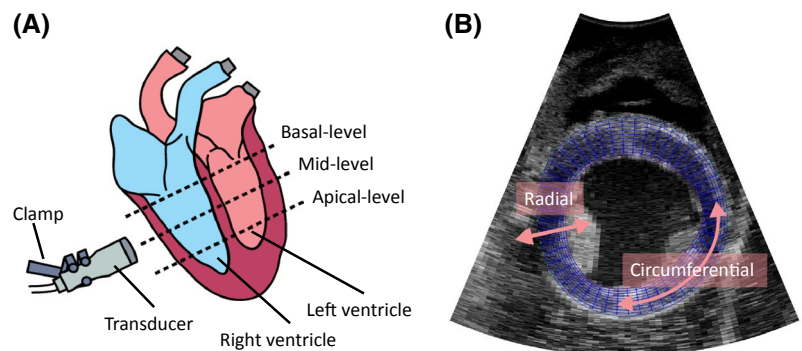
FIGURE 2 A, Diagram of the ex vivo heart showing ultrasound (US) transducer, clamp, and imaging planes. B, Representative US image at end-diastole showing the left ventricle at the level of the papillary muscles

(krpm), increasing in increments of 1 krpm. For each acquisition above 0 krpm, the MMD pump speed was 500 rpm higher than the HM2 LVAD (i.e., HM2 = 7 krpm, MMD = 7.5 krpm); this was due to preset manufacturer pump settings.

2.3 | Data analysis

2.3.1 | Strain estimation

RF data from the experiments were processed in MATLAB (version 2017a, The MathWorks Inc., Natick, MA, USA), using a strain imaging toolbox previously developed by Lopata et al.[26] The data were manually segmented into cine loops containing at least one heart cycle by using the M-mode of the center line through the left ventricle to visualize wall motion over each data sequence. Next, the lumen wall and outer wall boundaries of the myocardium in the first frame were manually segmented, and a mesh formed of 11 radial and 49 circumferential tracking points was generated. A "coarse-to-fine" 2-D displacement tracking algorithm was used to estimate per-frame displacements in the axial and lateral directions of the RF image data for the remaining frames in the cine loop. The intersecting points of the mesh were tracked based on the calculated displacements.

Circumferential (ε_{circ}) and radial (ε_{rad}) strains (indicated in Figure 2B) were estimated by taking the spatial derivative of the deformation of the mesh relative to the initial geometry, using a least squares strain estimator, in the true local strain directions.[26] The initial displacement estimates were then used to calculate LV cavity surface area over the sequence. The cavity surface area was the region of the LV bounded by the inner perimeter of the mesh, used due to the lack of LV volume measurements. Peak detection was applied, and two maxima were segmented as a single cardiac cycle beginning at end-diastole. The inner and outer walls of the myocardium were then manually resegmented. Time-to-peak strain was defined as the time taken from end-diastole for each point of the mesh to reach peak ε_{circ} over the heart cycle.

2.3.2 | Combining strain and hemodynamics

End-diastole and end-systole were defined as the points at which the cavity surface area was highest and lowest respectively. These points were selected due to the lack of an electrocardiogram (due to pacing) or views of the aortic valve. Aortic valve opening was defined as the time points at which LV pressure exceeded aortic pressure. The manually segmented end-diastolic geometry with no LVAD support (0krpm) was used as a reference geometry for each heart condition when calculating ε_{circ}.

Results of strain estimation were synchronized with concurrently measured pressures and flows. The minimum cavity surface area was automatically synchronized with the point of minimum LV pressure after aortic valve closure. A manual adjustment was made of up to two ultrasound samples, to account for errors in the synchronization due to different sample rates. Pressure–strain loops were created by plotting estimated ε_{circ} against measured LV pressure. The effects of pump speed and heart condition were compared through the analysis of the pressure–strain loops and loop area. Loop area is the product of strain (the relative change in length) and pressure and is given in units of mm Hg%.

3 | RESULTS

3.1 | Hemodynamic effect of pump speed & condition

Table 1 shows baseline hemodynamic measurements at 0 krpm, acquired over 20 heart cycles, for each heart. The porcine hearts remain stable within each hemodynamically defined heart condition, except for the latter conditions of Heart 2. The baseline condition of Hearts 1, 2, and 3 is similar while Heart 4 is already in a degraded state. A reduction in cardiac output is observed as each experiment progresses, reflected by the heart condition. In general, both aortic and LV pressure reduce with each successive heart condition. Heart 4 shows an increase in mean aortic pressure, mean LV pressure, and dP/dt$_{max}$ between conditions I and II. This was due to adjustments made to the preload and after-load of the mock circulatory loop to stabilize the heart. Differences in experimental time (ie, the number of conditions) and hemodynamic measurements occur due to either pre-existing biological differences in each porcine heart or as a result of any damage during preparation or reperfusion.

Figure 3 shows plots of pump speed against mean hemodynamic measurements acquired over 20 heart cycles, at each heart condition. Each measurement type declines with heart condition, except for pressure measurements in Heart 4. There is a small increase in mean aortic pressure and cardiac output with pump speed (mean difference from 0 to 10 krpm, mean aortic pressure = 0.592 mm Hg, CO = 0.414 L/min). LV pulse pressure and LV dP/dt$_{max}$ reduce as the pump speed is increased (mean difference of −31.1 mm Hg and −252.3 mm Hg, respectively). Circled points show pump speeds without aortic valve opening. The aortic valve always opened with pump speeds less than 9 krpm; only when degraded and under high load (9 & 10 krpm) did the valve close. LV pulse pressure and dP/dt$_{max}$ are markedly reduced during heart cycles where the aortic valve failed to open.

TABLE 1 Mean and standard deviation of hemodynamic measurements obtained at 0 krpm

Heart	Heart condition	MAoP [mm Hg]	CO [L/min]	LV pressure [mm Hg]	dP/dt$_{max}$ [mm Hg]	Heart rate [bpm]
1	I	85 ± 0.25	5.58 ± 0.03	62.4 ± 0.33	830 ± 2.3	120 ± 0.16
	II	81 ± 0.24	5.28 ± 0.06	57.5 ± 0.35	730 ± 8	120 ± 0.24
	III	78.2 ± 0.6	4.8 ± 0.04	54.7 ± 0.9	759 ± 15	120 ± 0.38
	IV	68.1 ± 0.51	3.66 ± 0.06	46.9 ± 0.47	632 ± 13	120 ± 0.25
2	I	74.9 ± 2.4	4.8 ± 0.05	55.2 ± 2.8	711 ± 39	133 ± 6.1
	II	67.7 ± 2	3.9 ± 0.18	50 ± 1.9	845 ± 38	120 ± 1.5
	III	59.2 ± 0.93	3.07 ± 0.08	44.6 ± 2.1	772 ± 18	120 ± 10
	IV	61.5 ± 0.29	3.02 ± 0.03	42.3 ± 0.19	803 ± 5.1	89.3 ± 0.4
3	I	73.4 ± 0.1	4.49 ± 0.02	49.2 ± 0.16	1.04×10^3 ± 1.9	118 ± 0.01
	II	58.6 ± 0.64	3 ± 0.05	44.1 ± 0.44	784 ± 15	121 ± 0.22
4	I	62.7 ± 0.17	3.12 ± 0.01	42 ± 0.13	624 ± 4.1	115 ± 0.29
	II	71.1 ± 0.16	2.9 ± 0.01	43.4 ± 0.14	609 ± 2.7	115 ± 0.1

Abbreviations: CO, cardiac output; dP/dt$_{max}$ maximum rate of LV pressure increase; LV pressure, mean left ventricular pressure; MAoP, mean aortic pressure.

3.2 | Ultrasound strain imaging

Figure 4 shows representative curves of ε_{circ} (upper section) and ε_{rad} (lower section) over individual cardiac cycles in one heart. As the hearts degrade and the pump speed is increased overall ε_{circ} magnitude increases; however, the range over the cycle reduces. The influence of pump unloading on strain can be shown as the pump speed is increased from 0 to 10 kprm: during condition I, mean ε_{circ} and ε_{circ} range reduce by −11.3 % and −1.44%, respectively, while during the final condition mean ε_{circ} reduces by −18.8% with mean ε_{circ} range reducing by −2.07%. At 10 krpm, mean ε_{circ} during the first condition is −15.3%, with a mean range of 6.70% over the cycle. During the final condition at 10 krpm, mean ε_{circ} is −21.5%, mean range 4.83%.

ε_{rad} measurements are noisier than ε_{circ} and show less obvious trends. Overall magnitude of strain decreases as the pump speed is increased, except at 10 krpm. ε_{rad} range shows a small reduction (difference in mean ε_{rad} range, condition I versus condition II/IV: 4.68% vs 4.36% at 0 krpm; 5.30% vs 4.94% at 10 krpm) as the heart degrades. Overall magnitude of peak ε_{rad} remains relatively unchanged as the hearts degrade and the pump speed is increased. There is no consistent difference between pump speeds or heart conditions.

3.3 | Pressure–strain loops

Figure 5 shows pressure–strain loops of estimated ε_{circ} against measured LV pressure over the cardiac cycle. In early conditions unloading has a minor effect on ventricular pressure and ε_{circ} as the pump speed is increased. Mean reduction in LV pressure between 0 and 10 krpm in the first condition is −24.0 mm Hg, LV pulse pressure reduces by −21.8 mm Hg. ε_{circ} range is not significantly affected as the pump speed is

increased when the hearts are healthy, although average strain magnitude increases. When in a degraded state pump unloading has a greater influence on ventricular pressure and ε_{circ}: mean LV pressure and LV pulse pressure reduce by −36.1 mm Hg and −46.8 mm Hg, respectively; mean ε_{circ} magnitude increases while the range reduces. Loops where the aortic valve does not open are triangular, with a sharp increase and decrease in LV pressure during ejection. Similarly, there is a sudden reduction in ε_{circ} at end-diastole when there is no aortic valve opening.

Figure 6 shows plots of pressure–strain loop area (in mm Hg%) against pump speed. Reducing heart condition leads to a progressive reduction in mean loop area at 0 krpm, from 519 to 323 mm Hg% in the first and final conditions, respectively. When the hearts are healthy, no reduction in area is seen as the pump speed is increased. When degraded, the hearts generally show a linear reduction in the loop area from baseline as the pump speed is increased. In condition I, mean loop area reduces from 519 to 325 mm Hg% between 0 and 10 krpm. In the final condition, mean loop area reduces from 323 to 52.5 mm Hg% between the same pump speeds.

3.4 | LVAD influence on contraction

Figure 7 shows B-mode images of the LV in Hearts 1 and 2 at end-diastole, overlaid with spatial plots of time-to-peak strain. Early peak strain (occurring at 0.1–0.2 seconds) is seen in the upper left portion of the LV. The area grows as the pump speed is increased and heart condition degrades. However, a region of later contraction occurring at 0.3–0.4 seconds in the inferior-septal region exists at lower pump speeds. Later peak strain occurring between 0.3 and 0.5 seconds is seen in the opposite (lateral) wall. After heart condition I, peak strain in this anterolateral region occurs later
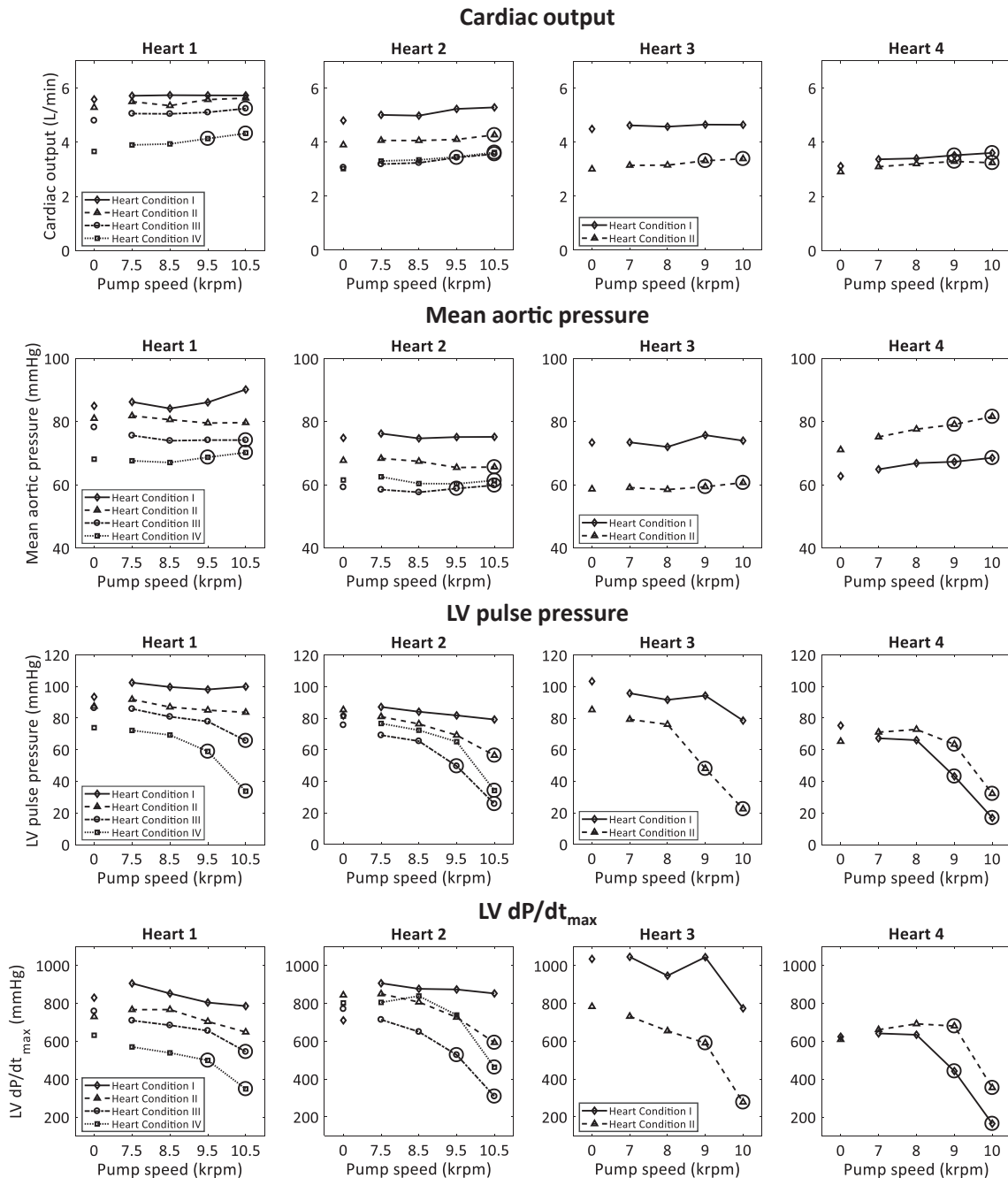
FIGURE 3 Plots of pump speed versus hemodynamic measurements at each pump speed and heart condition. First row, cardiac output; second row, mean aortic pressure; third row, left ventricular (LV) pulse pressure; fourth row, mean LV dP/dt$_{max}$. Circled points represent pump speeds where the aortic valve did not open

in the heart cycle as the pump speed increases. Peak strain occurs significantly later in Heart 4 condition IV than in the previous three conditions.

4 | DISCUSSION

The purpose of this study was to investigate the use of ultrasound strain imaging as a method to quantitate the effect of an LVAD on left ventricular mechanics over the cardiac cycle

and to provide information on the current ability of the LV to function. The method's utility was explored experimentally in ex vivo porcine hearts implanted with LVADs. Strain imaging showed the effect of LVAD unloading on the LV: The increase in circumferential strain magnitude with increased pump speed equates to a reduction in overall ventricular volume. The reduction in strain range as the hearts degraded shows the reduced ability of the heart to contract, especially at high pump speeds. Pressure–strain loops clearly showed the increasing influence of the pump through a reduction in
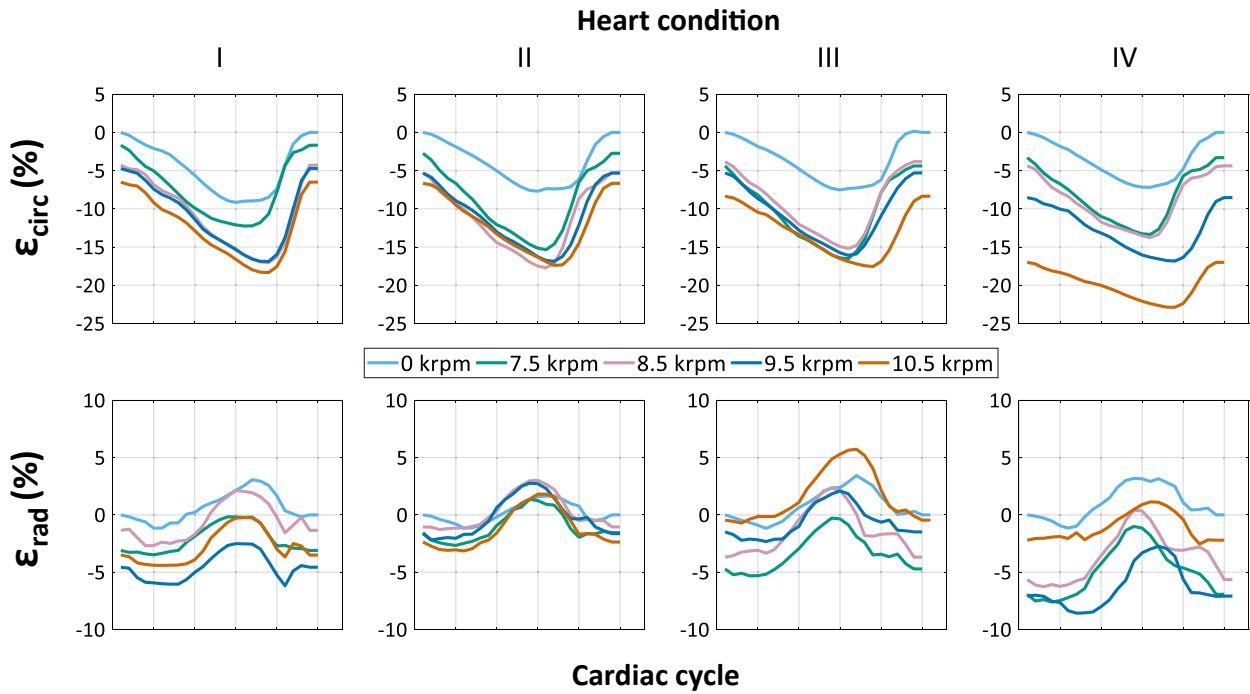
Heart condition

FIGURE 4 Representative curves of mean circumferential (ε_{circ}, upper) and radial (ε_{rad}, lower) strain over the cardiac cycle, for each pump speed in thousand revolutions per minute (krpm) and heart condition
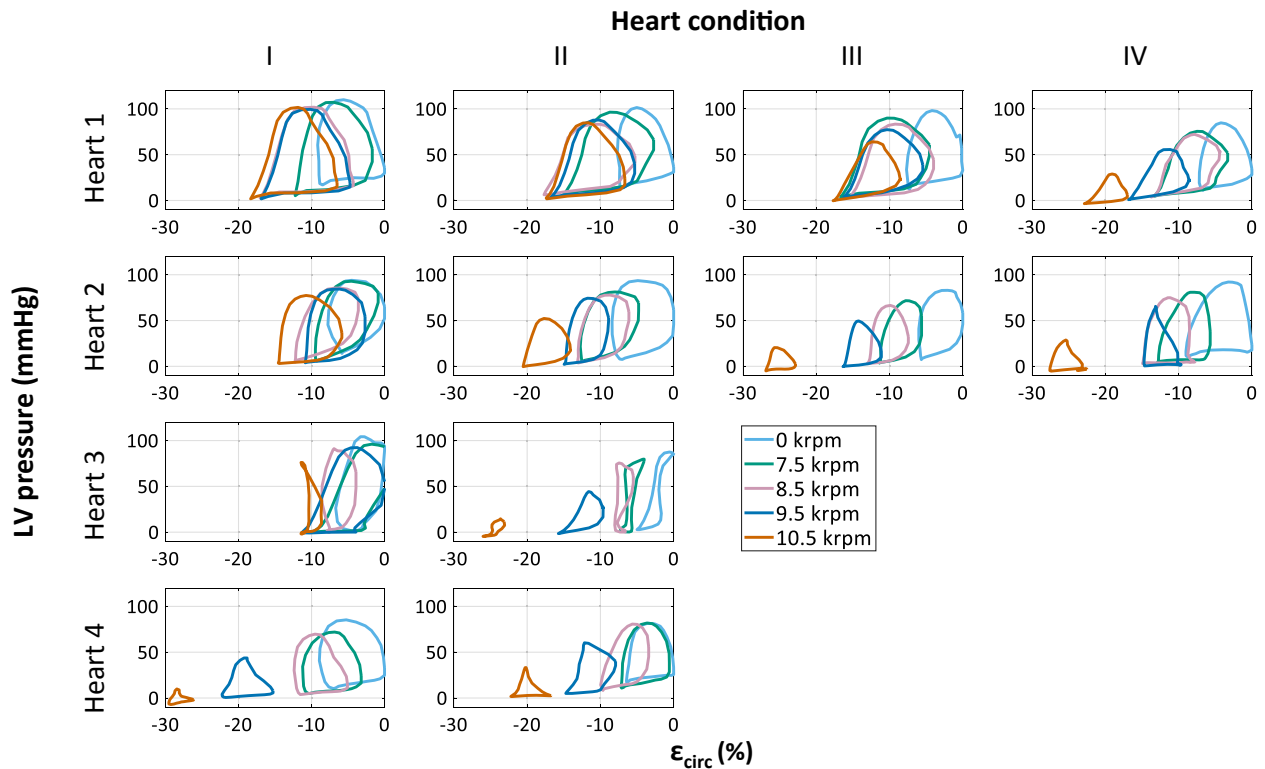
Heart condition

FIGURE 5 Pressure–strain loops at each pump speed in thousand revolutions per minute (krpm), in each heart and condition. LV, left ventricular; ε_{circ}, circumferential strain

loop area as the hearts degraded. Finally, it was shown that pump speed and degradation reduce the synchronicity of LV contraction.

As each experiment progressed, edema in the myocardium and an increase in waste products in the blood led to a reduction in the contractile function of each heart. This
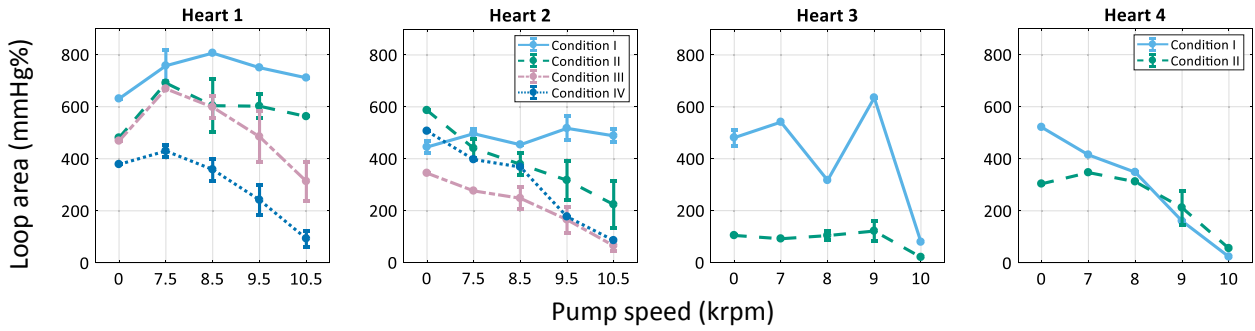
FIGURE 6 Pressure–strain loop area in each heart (in mm Hg%) for each heart condition and pump speed (in thousand revolutions per minute, krpm)
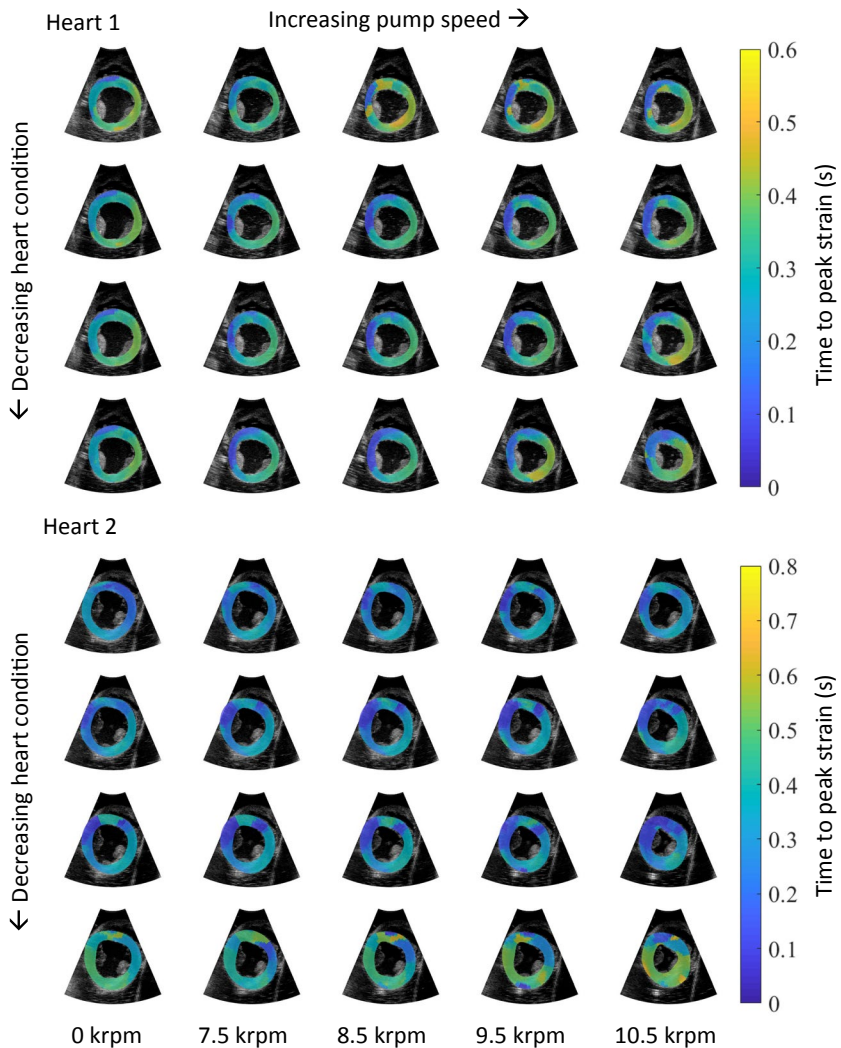

FIGURE 7 B-mode images at end-diastole overlaid with spatial plots of time-to-peak strain around the ventricle, with increasing pump speed and decreasing heart condition, ie, experimental time point

can be seen clearly in Figure 4 - in later heart conditions as the pump speed is increased, LV pulse pressure and dP/dt$_{max}$ are significantly reduced. Measurements of mean aortic pressure were within values reported by both Granegger et al and Pantalos et al[18,27] in similar mock loop experiments. Figure 3 shows that the aortic valve was only ever closed at 9 and 10 krpm, and in a degraded state. When aortic valve opening occurred the overall LV pressure was

higher; this influenced estimated strain over the heart cycle as seen in Figures 4 and 5.

With increasing pump speed and reduced heart condition, we observed an increase in circumferential strain magnitude, a reduced range in circumferential strain, and a reduction in overall left ventricular pressure over each cardiac cycle. This equates to a reduced cavity volume and a reduction in stroke volume. Radial strains were not indicative of changes

in ventricular loading from the LVAD; this is likely due to problems tracking displacements in the thin LV wall. Radial strain was heavily influenced by small variations in the manually segmented geometry; therefore, no reference geometry was used in radial strain calculations.

The pressure–strain loops show the increasing influence of the pump with the degradation of the hearts, as well as the static load imparted by continuous-flow LVADs. The change in loop shape and area due to LVAD unloading in our measurements is a known effect and has been shown previously in simulated pressure–volume loops[28] and those obtained invasively in animals.[29] In comparison to these studies, we obtained similar results using partially noninvasive methods (ultrasound). Pressure–strain loops have been investigated as a tool to quantitate regional myocardial work in cardiac resynchronization therapy patients[22] and myocardial work during ejection in a population sample.[23] The contribution of our study to wider research on pressure–strain loops is by showing that the immediate influence of different loading conditions on LV function can be measured through their use.

Initial in vivo patient measurements are an important next step in the development and validation of the methods used in this study. This will present a challenge given that invasive LV pressure measurements are not possible. Recent studies have estimated LV pressure from brachial pressure and by adapting reference measurements,[22,23] while others have demonstrated the in vivo feasibility of measuring pressure via implanted cardiac devices, including LVADs.[30,31] Consequently, direct LV pressure measurements may become available for use in future clinical studies.

Changes in contraction pattern with pump speed and heart condition were observed through regional time-to-peak strain. LVAD unloading changes the shape of the left ventricle by moving the septum inward at high flow rates and altering the contraction pattern of the ventricle. This is relevant in terms of remaining LV function given that a nonuniform contraction will be less efficient during ejection.

The lack of relaxation in the hearts as they degrade, combined with the presence of edema, shows that the hearts are failing in the diastolic phase of the cardiac cycle (Figure 5). When healthy, LV contraction is relatively normal despite the continuous unloading from the pump, given the consistent loop area. When degraded and being unloaded by the pump, there is less ventricular filling (especially at high pump speeds), as the LV is unable to relax during diastole due to the stiffening and weakening myocardium. This is shown by the marked reduction in the loop area.

4.1 | Limitations

2-D ultrasound was used to acquire short-axis images of the left ventricle. Much of the contraction of the ventricle occurs in the longitudinal plane. This is a large source of error in our displacement estimates, as image features being tracked can move out of the imaging plane. The presence of LVAD prevented the use of the longitudinal parasternal or four-chamber views in our analysis. In off-axis longitudinal views the LVAD cannula often shifted into the view. Apical views available in patient's postimplantation are foreshortened as the probe must also be oriented off-axis, leading to unreliable strain estimates. To our best knowledge there have been no studies reporting strain in the apical four-chamber view post-LVAD implantation.

RF data were obtained at 47 Hz with an average of 24 frames per heart cycle. For an accurate estimation of the global strain, a minimum of 30 frames per cycle is needed.[32] In our experiments we were limited by the hardware used and the wide aperture and large depth required to image the entire LV. Image quality is reduced in patients due to the greater imaging depth required and attenuating structures such as the ribs. This negatively affects strain estimation. This can be mitigated somewhat with higher ultrasound acquisition rates and by regularizing displacement estimates. It must be noted that the pressure–strain loops only provide a relative measure of LV function; in the present study this was relative to the 0-krpm pump speed for each heart condition. Finally, a major limitation of our study was the use of only four hearts along with two different LVAD variants.

4.2 | Future work

In future ex vivo studies 3-D and higher frame rate ultrasound acquisition methods could be employed to account for some of the limitations of this study. This would enable more precise tracking of displacements and estimation of strains that currently occur outside the imaging plane. The estimation or measurement of left ventricular pressure is required for use of pressure–strain loops in any future study in patients. Eventual utility of the methods presented in this study would primarily be of use in optimizing pump speed settings for "bridge-to-recovery" patient scenarios, where any deterioration or improvement in residual LV function is of utmost importance.

5 | CONCLUSION

In this study we investigated the use of ultrasound strain imaging for the determination of left ventricular function in the LVAD-supported heart. We have demonstrated that through the analysis of both pressure and strain the current ability of the heart to perform work while undergoing LVAD support can be understood. Pressure–strain loop shape and area are indicative of the remaining function. These results are a step toward a direct method to estimate remaining heart function in LVAD patients.

CONFLICT OF INTEREST

The authors declare no conflict of interest that might have influenced the (presentation of the) work described in this manuscript.

ORCID

Louis S. Fixsen 🅤 https://orcid.org/0000-0001-5191-3502
Niels J. Petterson 🅤 https://orcid.org/0000-0002-9339-3071
Richard G. P. Lopata 🅤 https://orcid.org/0000-0001-6618-6184

REFERENCES

1. Feldman D, Pamboukian SV, Teuteberg JJ, Birks E, Lietz K, Moore SA, et al. The 2013 international society for heart and lung transplantation guidelines for mechanical circulatory support: executive summary. J Heart Lung Transplant. 2013 Feb;32:157–87.

2. Topkara VK, Garan AR, Fine B, Godier-Furnémont AF, Breskin A, Cagliostro B, et al. Myocardial recovery in patients receiving contemporary left ventricular assist devices: results from the interagency registry for mechanically assisted circulatory support (INTERMACS). Circ Heart Fail [Internet]. 2016 Jul [cited 2019 Apr 17];9. Available from: https://www.ahajournals.org/doi/10.1161/CIRCHEARTFAILURE.116.003157

3. Jakovljevic DG, Yacoub MH, Schueler S, MacGowan GA, Velicki L, Seferovic PM, et al. Left ventricular assist device as a bridge to recovery for patients with advanced heart failure. J Am Coll Cardiol. 2017 Apr;69:1924–33.

4. Lietz K, Long JW, Kfoury AG, Slaughter MS, Silver MA, Milano CA, et al. Outcomes of left ventricular assist device implantation as destination therapy in the post-REMATCH era: implications for patient selection. Circulation. 2007;116:497–505.

5. Park SJ, Milano CA, Tatooles AJ, Rogers JG, Adamson RM, Steidley DE, et al. Outcomes in advanced heart failure patients with left ventricular assist devices for destination therapy. Circ Heart Fail. 2012;5:241–8.

6. Uriel N, Morrison KA, Garan AR, Kato TS, Yuzefpolskaya M, Latif F, et al. Development of a novel echocardiography ramp test for speed optimization and diagnosis of device thrombosis in continuous-flow left ventricular assist devices: the Columbia ramp study. J Am Coll Cardiol. 2012;60:1764–75.

7. Slaughter MS, Pagani FD, Rogers JG, Miller LW, Sun B, Russell SD, et al. Clinical management of continuous-flow left ventricular assist devices in advanced heart failure. J Heart Lung Transplant. 2010;29(4 Suppl.):S1–39.

8. Rear R, Bell RM, Hausenloy DJ. Contrast-induced nephropathy following angiography and cardiac interventions. Heart. 2016 Apr;102:638–48.

9. Raina A, Seetha Rammohan HR, Gertz ZM, Rame JE, Woo YJ, Kirkpatrick JN. Postoperative right ventricular failure after left ventricular assist device placement is predicted by preoperative echocardiographic structural, hemodynamic, and functional parameters. J Card Fail. 2013;19:16–24.

10. Chapman CB, Allana S, Sweitzer NK, Kohmoto T, Murray M, Murray D, et al. Effects of the HeartMate II left ventricular assist device as observed by serial echocardiography. Echocardiography. 2013;30:513–20.

11. Myers TJ, Frazier OH, Mesina HS, Radovancevic B, Gregoric ID. Hemodynamics and patient safety during pump-off studies of an axial-flow left ventricular assist device. J Heart Lung Transplant. 2006;25:379–83.

12. Hatano M, Kinugawa K, Shiga T, Kato N, Endo M, Hisagi M, et al. Less frequent opening of the aortic valve and a continuous flow pump are risk factors for postoperative onset of aortic insufficiency in patients with a left ventricular assist device. Circ J. 2011;75:1147–55.

13. Toda K, Fujita T, Domae K, Shimahara Y, Kobayashi J, Nakatani T. Late aortic insufficiency related to poor prognosis during left ventricular assist device support. Ann Thorac Surg. 2011;92:929–34.

14. Langeland S, D'Hooge J, Wouters PF, Leather HA, Claus P, Bijnens B, et al. Experimental validation of a new ultrasound method for the simultaneous assessment of radial and longitudinal myocardial deformation independent of insonation angle. Circulation. 2005 Oct;112:2157–62.

15. Amundsen BH, Helle-Valle T, Edvardsen T, Torp H, Crosby J, Lyseggen E, et al. Noninvasive myocardial strain measurement by speckle tracking echocardiography: validation against sonomicrometry and tagged magnetic resonance imaging. J Am Coll Cardiol. 2006 Feb;47:789–93.

16. Bertola B, Rondano E, Sulis M, Sarasso G, Piccinino C, Marti G, et al. Cardiac dyssynchrony quantitated by time-to-peak or temporal uniformity of strain at longitudinal, circumferential, and radial level: implications for resynchronization therapy. J Am Soc Echocardiogr. 2009 Jun;22:665–71.

17. Gupta DK, Skali H, Rivero J, Campbell P, Griffin L, Smith C, et al. Assessment of myocardial viability and left ventricular function in patients supported by a left ventricular assist device. J Heart Lung Transplant. 2014;33:372–81.

18. Pantalos GM, Koenig SC, Gillars KJ, Giridharan GA, Ewert DL. Characterization of an adult mock circulation for testing cardiac support devices. ASAIO J. 2004;50:37–46.

19. Leopaldi AM, Vismara R, van Tuijl S, Redaelli A, van de Vosse FN, Fiore GB, et al. A novel passive left heart platform for device testing and research. Med Eng Phys. 2015;37:361–6.

20. Pennings KAMA, van Tuijl S, van de Vosse FN, de Mol BAJ, Rutten MCM. Estimation of left ventricular pressure with the pump as "sensor" in patients with a continuous flow LVAD. Int J Artif Organs. 2015;38:433–43.

21. Petterson NJ, Fixsen LS, Rutten MCMM, Pijls NHJJ, Van De Vosse FN, Lopata RGPP. Ultrasound functional imaging in an ex vivo beating porcine heart platform. Phys Med Biol. 2017;62:9112–26.

22. Russell K, Eriksen M, Aaberge L, Wilhelmsen N, Skulstad H, Remme EW, et al. A novel clinical method for quantification of regional left ventricular pressure–strain loop area: a non-invasive index of myocardial work. Eur Heart J. 2012 Mar;33:724–33.

23. Cauwenberghs N, Tabassian M, Thijs L, Yang W-Y, Wei F-F, Claus P, et al. Area of the pressure–strain loop during ejection as non-invasive index of left ventricular performance: a population study. Cardiovasc Ultrasound [Internet]. 2019 Dec [cited 2019 Sep

15];17. Available from: https://cardiovascularultrasound.biomedcentral.com/articles/10.1186/s12947-019-0166-y.

24. de Hart J, de Weger A, van Tuijl S, Stijnen JMA, van den Broek CN, Rutten MCM, et al. An ex vivo platform to simulate cardiac physiology: a new dimension for therapy development and assessment. Int J Artif Organs. 2011;34:495–505.

25. Schampaert S, van Nunen LX, Pijls NHJ, Rutten MCM, van Tuijl S, van de Vosse FN, et al. Intra-aortic balloon pump support in the isolated beating porcine heart in nonischemic and ischemic pump failure: IABP support in (non)ischemic pump failure. Artif Organs. 2015 Nov;39:931–8.

26. Lopata RGP, Hansen HHG, Nillesen MM, Thijssen JM, De Korte CL. Comparison of one-dimensional and two-dimensional least-squares strain estimators for phased array displacement data. Ultrason Imaging. 2009 Jan;31:1–16.

27. Granegger M, Aigner P, Haberl T, Mahr S, Tamez DA, Graham J, et al. Interaction of a transapical miniaturized ventricular assist device with the left ventricle: hemodynamic evaluation and visualization in an isolated heart setup. Artif Organs. 2016;40:1113–20.

28. Bozkurt S, Safak KK. Evaluating the hemodynamical response of a cardiovascular system under support of a continuous flow left ventricular assist device via numerical modeling and simulations. Comput Math Methods Med. 2013;2013:1–12.

29. Bartoli CR, Giridharan GA, Litwak KN, Sobieski M, Prabhu SD, Slaughter MS, et al. Hemodynamic responses to continuous versus pulsatile mechanical unloading of the failing left ventricle. ASAIO J. 2010 Sep;56:410–6.

30. Hubbert L, Baranowski J, Delshad B, Ahn H. Left atrial pressure monitoring with an implantable wireless pressure sensor after implantation of a left ventricular assist device. ASAIO J. 2017;63:e60–5.

31. Gregory SD, Stevens MC, Pauls JP, Schummy E, Diab S, Thomson B, et al. Vivo evaluation of active and passive physiological control systems for rotary left and right ventricular assist devices. In vivo evaluation of physiological control systems. Artif Organs. 2016 Sep;40:894–903.

32. Rösner A, Barbosa D, Aarsæther E, Kjønås D, Schirmer H, D'Hooge J. The influence of frame rate on two-dimensional speckle-tracking strain measurements: a study on silico-simulated models and images recorded in patients. Eur Heart J Cardiovasc Imaging. 2015;16:1137–47.